Provided for non-commercial research and education use.
Not for reproduction, distribution or commercial use.

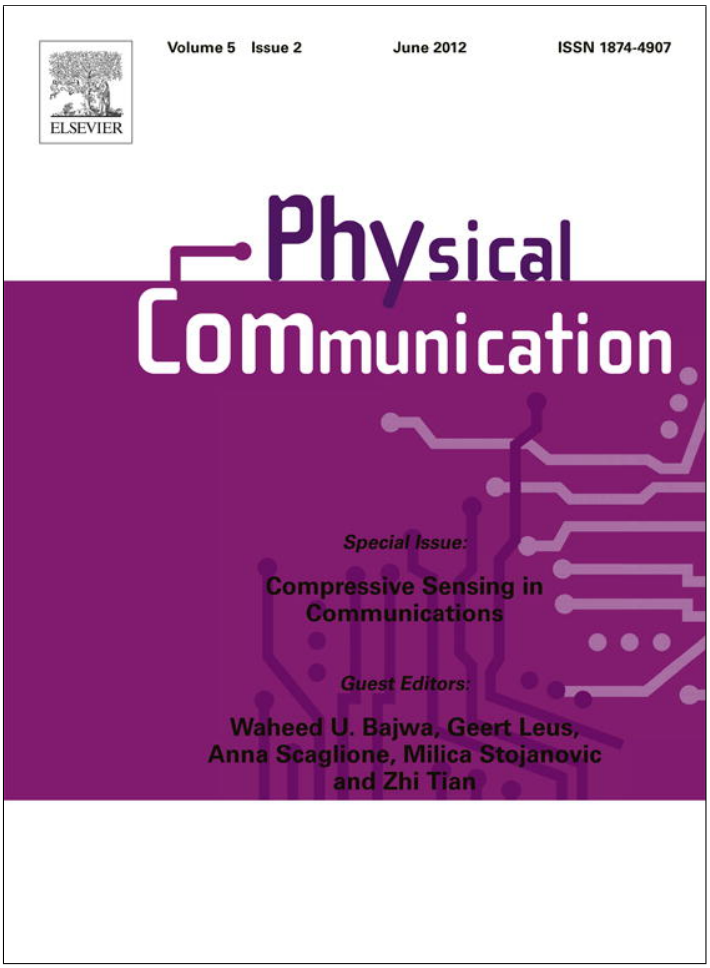

This article appeared in a journal published by Elsevier. The attached copy is furnished to the author for internal non-commercial research and education use, including for instruction at the authors institution and sharing with colleagues.

Other uses, including reproduction and distribution, or selling or licensing copies, or posting to personal, institutional or third party websites are prohibited.

In most cases authors are permitted to post their version of the article (e.g. in Word or Tex form) to their personal website or institutional repository. Authors requiring further information regarding Elsevier's archiving and manuscript policies are encouraged to visit:

http://www.elsevier.com/copyright

Author's personal copy

Physical Communication 5 (2012) 148–160

Contents lists available at SciVerse ScienceDirect

Physical Communication

journal homepage: www.elsevier.com/locate/phycom

Full length article

Compressed sensing in random access networks with applications to underwater monitoring☆

Fatemeh Fazel [a,*], Maryam Fazel [b], Milica Stojanovic [a]

[a] Department of Electrical and Computer Engineering, Northeastern University, Boston, MA, 02115, United States

[b] Department of Electrical Engineering, University of Washington, Seattle, WA, 98195, United States

ARTICLE INFO

Article history:
Received 21 December 2010
Received in revised form 29 June 2011
Accepted 9 September 2011
Available online 22 September 2011

Keywords:
Sensor networks
Compressed sensing
Wireless communications
Underwater acoustic networks
Random access

ABSTRACT

For networks that are deployed for long-term monitoring of environmental phenomena, it is of crucial importance to design an efficient data gathering scheme that prolongs the lifetime of the network. To this end, we consider a Random Access Compressed Sensing (RACS) scheme that considerably reduces the power and bandwidth usage of a large network. Motivated by underwater applications, we propose a continuous-time RACS that eliminates the need for synchronization and scheduling which are difficult to achieve in a distributed acoustic network. We provide an analytical framework for system design that ensures fast recovery and power-efficiency. Through analysis and examples, we demonstrate that recovery of the field can be attained using only a fraction of the resources used by a conventional TDMA network, while employing a scheme which is simple to implement.

© 2011 Elsevier B.V. All rights reserved.

1. Introduction

With the advances in underwater sensor technology, it is envisioned that underwater sensor networks, consisting of a number of static or mobile nodes, will be deployed to monitor physical, chemical or biological phenomena in the ocean. Potential applications of underwater sensor networks are in environmental observation and data collection (e.g., temperature, salinity, oxygen levels, pollutants, etc.), field and equipment monitoring (e.g., in deep-sea oil-fields) or disaster prevention [1]. Wireless acoustic communication is the physical layer technology used in underwater networking. Three main characteristics distinguish an acoustic communication system from its radio counterpart: limited and distance-dependent bandwidth, time-varying multipath propagation, and high latency. The shortage in bandwidth results in long packets, thus increasing the probability of packet collision in contention-based medium access protocols. Due to the low speed of sound, the propagation delay in acoustic communication could be comparable to the packet duration. This fact calls for careful scheduling, especially when deterministic medium access methods such as time division multiple access (TDMA) are employed. Additionally, recharging batteries in sensor devices that are deployed underwater is difficult.

In this paper, we consider a static area network, where sensor nodes are anchored to the sea floor, and deployed for long periods of time (months or even years). Each sensor node communicates its observations to a central node, referred to as the fusion center (FC) and the FC reconstructs the map of the field of interest. To be able to operate over long intervals of time, sensor nodes need to conserve their energy. In both wireless networks and underwater acoustic networks, power consumption is a major concern. A large body of literature examines energy-aware design methodologies for managing the periodic sleep cycles of sensors, such as [2–4]. Furthermore, bandwidth is severely limited in underwater acoustic networks, hence efficient networking schemes are of particular importance [5,6].

To achieve the desired efficiency, we capitalize on the fact that most natural phenomena are sparse (compress-

☆ Research funded in part by ONR grant N00014-09-1-0700, NSF grant 0831728 and NSF CAREER grant ECCS-0847077.

* Corresponding author.
E-mail address: fatemeh.fazel@gmail.com (F. Fazel).

1874-4907/$ – see front matter © 2011 Elsevier B.V. All rights reserved.
doi:10.1016/j.phycom.2011.09.003

Author's personal copy

ible) in an appropriate basis and exploit the principle of compressed sensing. The theory of compressed sensing establishes that under certain conditions, exact signal recovery is possible with a relatively small number of random measurements [7,8]. Application of compressed sensing in wireless sensor networks was first introduced in [9–11], where the authors use phase-coherent transmission of randomly-weighted data from sensor nodes to the FC over a dedicated multiple-access channel, to form distributed projections of data onto an appropriate basis at the FC. In this approach sensors need to be perfectly synchronized, which is difficult to maintain in underwater acoustic networks. Ref. [12] proposes compressive cooperative spatial mapping using mobile sensors based on a small set of observations. A number of references, such as [13,14], focus on phenomena that are sparse in the spatial domain, e.g., event detection or tracking of multiple targets. In [15], authors consider a decentralized network (without FC), where active nodes exchange measurements locally. The authors formulate sparse recovery as a decentralized consensus optimization problem and show that their iterative decentralized algorithm converges to a globally optimal solution. In [16], ultra-low power infrastructure monitoring is achieved by employing data compression and a low-collision MAC protocol. Authors in [17,18] consider spatial mapping using mobile sensors (robots) and show that if robots cover the field in a random path, reconstruction can be achieved with far fewer samples. Finally, in [19], capacity bounds of an on–off random multiple access channel are determined by transforming the problem to an equivalent compressed sensing problem and using the sparsity detection algorithms.

Employing the principles of compressed sensing and random channel access, in [20], we proposed a simple and efficient networking scheme referred to as *Random Access Compressed Sensing* (RACS). The RACS scheme consists of distributed random sampling, followed by random channel access. The key idea behind RACS is that packet collisions (which are inevitable in random access) occur randomly and thus do not change the random nature of the observations provided to the FC. Since the FC only needs to receive some, and not all the sensor packets, it can simply disregard the collisions. By disregarding collisions, we eliminate the need for listening to the medium (as used in contention-based MAC protocols), which in turn reduces the energy consumption of sensor nodes. The FC obtains an incomplete set of measurements (due to both random sensing and losses due to random access) from which it reconstructs the field using compressed sensing techniques. To provide a sufficient number of measurements to the FC, we compensate for the collision losses by initially selecting the number of participating sensors to be somewhat greater than the minimum number of packets required.

The RACS scheme [20] assumes a frame-based (slotted) transmission and batch reconstruction, i.e., the sampling process is performed at the beginning of a frame, the FC collects data within one frame duration, and at the end of each frame it attempts to reconstruct the field. Once the reconstruction is performed, the frame is discarded and the FC waits for a new set of data in the next frame. The frame-based RACS requires the sensor nodes to be synchronized, which is challenging in large acoustic networks where variable propagation delays are present and the nodes are subject to clock drift. This fact motivates our present work, whose goal is to dispense with synchronization and scheduling requirements.

We propose a continuous-time networking scheme that employs the RACS principles yet obviates the need for frame-based transmission. For such a scheme, we develop an analytical model for the data collection process that provides the system designer with a flexible tool to trade-off the recovery time for power-efficiency. The proposed continuous-time RACS has a simple implementation and eliminates the need for time-synchronization.

The rest of the paper is organized as follows. In Section 2, we introduce the network model, discuss the application of compressed sensing to our problem, and review the RACS scheme [20]. In Section 3, we propose two analytical frameworks to model the continuous transmission of data. In Section 4, we offer two design approaches to determine the network parameters. In Section 5, we analyze the performance of the proposed system in terms of power consumption and bandwidth requirements, and compare it with a conventional TDMA network. Section 6 illustrates the performance of the suggested scheme on a sample data set. Finally, we provide the concluding remarks in Section 7.

Notations: We denote by ℓ_p the p-norm of a vector $\mathbf{x} = [x_1, \ldots, x_N]^T$, $\|\mathbf{x}\|_{\ell_p} = \left(\sum_{i=1}^{N} |x_i|^p\right)^{1/p}$. If $\mathbf{V}$ is a $k \times l$ matrix, vec($\mathbf{V}$) denotes the $kl \times 1$ vector formed by stacking the columns of matrix $\mathbf{V}$, in other words, $\text{vec}(\mathbf{V}) = \begin{bmatrix} v_{11} & \ldots & v_{l1} & \ldots & v_{1k} & \ldots & v_{lk} \end{bmatrix}^T$. We denoteby $B(N, p)$ the binomial probability distribution of the number of successes in a sequence of N independent experiments, each of which has a success probability p. Finally, $\mathbf{A} \otimes \mathbf{B}$ denotes the Kronecker product of matrices $\mathbf{A}$ and $\mathbf{B}$.

2. Random access compressed sensing network model

Consider a grid network shown in Fig. 1, which consists of $N = IJ$ sensors located on a two-dimensional plane, with J and I sensors in x and y directions, respectively. The sensors are separated by distance d in each direction. The total coverage area of the network is $A = Nd^2$. We assume that the network has the task of measuring a physical phenomenon, $u(x, y, t)$, whose coherence time is T_{coh}. At time t, the sensor node located at position (i, j) in the network grid acquires a measurement denoted by $u_{ij}(t) = u(x_j, y_i, t)$, where $i \in \{1, \ldots, I\}$ and $j \in \{1, \ldots, J\}$ and x_j and y_i denote the sensor's position in the two-dimensional space. Note that the process is slowly varying during T_{coh}, thus we can assume that $u_{ij}(t_1) \approx u_{ij}(t_2)$ for $|t_1 - t_2| \leq T_{coh}$. In what follows, we will focus on an observation window of size $T \leq T_{coh}$, and drop the time index from the sensor measurements.

The measurements are sent to the FC whose task is to reconstruct the field of interest. For example, the FC can be located on the surface of a body of water with depth D, as shown in Fig. 2, such that node n is at a distance D_n from the

Author's personal copy

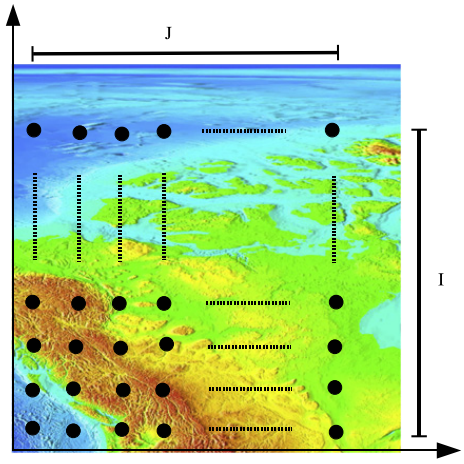

Fig. 1. A grid sensor network consisting of $N = IJ$ sensor nodes.

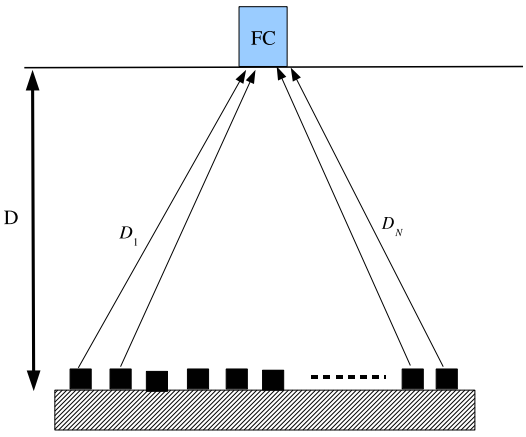

Fig. 2. Positioning of the fusion center on the surface.

FC, for $n \in \{1, \ldots, N\}$. The complete map of the process, obtained by the sensor measurements, is denoted by

$$\mathbf{U} = \left[u_{ij}\right]_{\substack{i=1,\ldots,I \\ j=1,\ldots,J}} . \tag{1}$$

Most natural phenomena have a compressible (sparse) representation in the frequency domain [18,12], and we will assume that this holds for our measurements as well. Specifically, let $\mathbf{V} = \mathbf{W}_I \mathbf{U} \mathbf{W}_J$ be the two-dimensional spatial discrete Fourier transform of $\mathbf{U}$, where $\mathbf{W}_I$ is the matrix of discrete Fourier transform coefficients, $\mathbf{W}_I[m, k] = e^{-j2\pi mk/I}$. It can now be shown that $\mathbf{v} = (\mathbf{W}_J \otimes \mathbf{W}_I)\mathbf{u}$, where $\mathbf{v} = \mathrm{vec}(\mathbf{V})$ and $\mathbf{u} = \mathrm{vec}(\mathbf{U})$. The Fourier representation, $\mathbf{v}$, is assumed to be sparse.

Each sensor node measures the physical quantity of interest and encodes the measurements, along with the sensor's location tag, into a data packet of L bits, which is then transmitted to the FC. Upon receiving a data packet, the FC demodulates the signal and extracts the measurement information as well as the location information of the transmitting sensor. If each sensor is given a fixed bandwidth B to communicate with the FC, the packet duration is $T_p = \frac{L}{B}$, where we assume without the loss of generality that the bandwidth is equal to the bit rate. The propagation delay of each packet depends on the distance between the sensor node and the FC, i.e., the propagation delay of node n's packet is given by $\tau_n = \frac{D_n}{c}$, where $c = 1500$ m/s is the nominal speed of sound underwater. The observations of a random subset of M sensors' packets at the FC can be expressed as

$$\mathbf{y} = \mathbf{R}\mathbf{u} + \mathbf{z} \tag{2}$$

where $\mathbf{R}$ is an $M \times N$ random selection matrix, consisting of M rows of the identity matrix selected at random, and $\mathbf{z}$ represents the measurement noise. Note that the communication noise translates into bit errors; in this work, we neglect the communication noise and assume that packets are received error-free. Note that each row of the matrix $\mathbf{R}$ contains a single 1 at the position of a received packet while all the other elements are zero. The FC can simply form the random selection matrix $\mathbf{R}$ from the received packets, since the location information of the transmitting node is encoded in the packet.

Noting that $\mathbf{u} = \mathbf{\Psi}\mathbf{v}$, where $\mathbf{\Psi} = (\mathbf{W}_J \otimes \mathbf{W}_I)^{-1}$ is the Inverse Discrete Fourier Transform (IDFT) matrix, Eq. (2) can be re-written in terms of the sparse vector $\mathbf{v}$ as follows

$$\mathbf{y} = \mathbf{R}\mathbf{\Psi}\mathbf{v} + \mathbf{z}. \tag{3}$$

To reconstruct the field, the FC first tries to recover the vector $\mathbf{v}$ as accurately as possible, then uses it to construct the map $\mathbf{U}$. Given the observations $\mathbf{y}$, the random selection pattern $\mathbf{R}$ and the sparsity basis $\mathbf{\Psi}$, and in the absence of noise – which is the case we will be focusing on – reconstruction can be performed by solving the following minimization problem:

$$\text{minimize}_{\tilde{\mathbf{v}}} \ \ \|\tilde{\mathbf{v}}\|_{\ell_1} \quad \text{subject to } \mathbf{R}\mathbf{\Psi}\tilde{\mathbf{v}} = \mathbf{y}. \tag{4}$$

The theory of compressed sensing (specifically, [21]) states that as long as the number of observations, picked uniformly at random, is greater than $CS \log N$, then with very high probability the solution to the convex optimization problem (4) is unique and is equal to $\mathbf{v}$. Here C is a constant that is independent of N and S (see [21] for the details). Thus, in our case, it suffices to ensure that the FC collects at least $N_s = CS \log N$ packets picked uniformly at random from different sensors to guarantee accurate reconstruction of the field with very high probability.

2.1. Frame-based RACS

In the frame-based transmission [20], we assume that all the sensor nodes are time-synchronized, i.e., that every node knows when a data frame begins at the FC. This can be achieved by employing a synchronization algorithm such as [22] or by having the FC broadcast a beacon signal which the nodes then use to time their transmissions. At frame k, a random subset of sensors is selected to conduct measurements. This can be done in a distributed manner by equipping the sensors with independent, identically distributed Bernoulli random generators, i.e., by having each sensor toss an identical coin. At the beginning of a frame, each node determines whether it will participate in the sensing process, which occurs with some probability p. The selected nodes then use random channel access to transmit their data to the FC. Specifically, sensor n picks a random transmission delay θ_n uniformly in $[0, T - T_p]$, where $T \leq T_{coh}$ is the frame duration.

Author's personal copy

As in any random access, packets may collide at the FC. The key idea here is to let the FC simply discard the colliding packets. This approach is motivated by the compressed sensing theory and the fact that the FC does not care *which* specific sensors are selected as long as (i) the selected subset is chosen uniformly at random, and (ii) there are sufficiently many collision-free packets received at the FC to allow for the reconstruction of the field. Therefore, once a collision is detected, the FC simply discards the colliding packets and reconstructs the data using the rest of the packets. Note that the matrix **R** of Eq. (3) now includes both the effects of random selection and random collisions. The frame-based RACS scheme [20] is summarized below:

Step 1. At the beginning of a frame, sensor node n tosses a coin to determine whether it participates in sensing (with probability p) or stays inactive (with probability $1-p$) during that frame.

Step 2. If node n is selected for sampling, it measures the physical quantity of interest and encodes it into a packet of L bits. The sensor's location is also included in the packet.

Step 3. Node n picks a uniformly-distributed delay for the transmission of its packet.

Step 4. FC collects the packets received during one frame. If a collision is detected, FC discards the colliding packets.

Step 5. At the end of the frame, FC uses the correctly received packets to form Eq. (3) and then reconstructs the data using ℓ_1 minimization in Eq. (4). We assume that packets which do not collide are correctly received.

3. Continuous transmission RACS

Maintaining time synchronization is a challenging task in large acoustic networks. First, due to the skew of the local clock at each sensor and the long deployment time of the network, synchronization process needs to be repeated frequently. Second, propagation delays are long and may vary with time as the channel conditions change. Both of these facts make network synchronization difficult and motivate the demand for schemes that can do without synchronization.

Continuous-time RACS that we describe here, is a simple and completely distributed networking scheme whose goal is to eliminate the need for synchronized scheduling. This scheme does not rely on time slotting, but the nodes instead transmit asynchronously, whenever they have a packet. We consider two packet generation processes for the distributed sensors: a deterministic, and a Poisson process. For each of these cases, we analyze the aggregate arrival process of the *useful* packets at the FC, and study the conditions under which this process yields a sufficient number of measurements, $N_s = CS\log N$. These conditions in turn imply a *per-node packet generation rate*, λ_1, or *a collection time*, T, that meets the system requirements. These two parameters completely define a continuous-time RACS system.

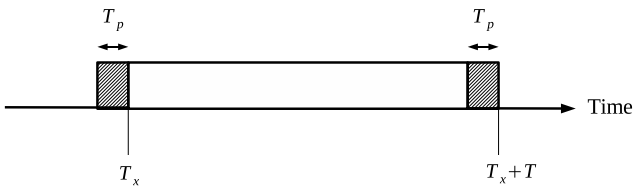

Fig. 3. FC collects the received packets within an interval $[T_x, T_x+T]$.

3.1. Scenario 1: deterministic arrival process

In this scenario, each node senses the field every T_1 seconds, and transmits its packets as soon as it is generated. However, the nodes are not synchronized, and the FC perceives the data packets as being generated at different (uniformly random) instants within $[0, T_1]$. In other words, according to the FC's clock, packet n is generated at time t'_n and arrives at the FC at time $t_n = t'_n + \tau_n$, where τ_n is the propagation delay of node $n \in \{1, \ldots, N\}$.

The FC starts collecting the packets at time T_x and collects the received packets within an observation interval of duration T, as shown in Fig. 3. Note that the packets that arrive after $T_x + T - T_p$ will not have been completed by the end of the collection window; hence, they are not counted in the number of received packets. Packets that arrive in $[T_x - T_p, T_x]$ are not within the collection window, yet they can cause collision to data packets, and as such have to be taken into account when calculating the number of collisions. The FC needs to recover the field in $T \le T_{coh}$, before the sensing field has undergone considerable change. The probability that a full packet from sensor n arrives within duration T is given by

$$\text{prob}\left(T_x \le t_n \le T_x + T - T_p\right) = \lambda_1(T - T_p) \tag{5}$$

where $\lambda_1 = 1/T_1$ is the per-node packet generation rate and t_n is the arrival time of sensor n's packet. Given that packet n has arrived at time t_n, a collision will occur if another packet m arrives at any time in $[t_n - T_p, t_n + T_p]$. This event occurs with the probability

$$\text{prob}\left(t_n - T_p \le t_m \le t_n + T_p\right) = 2\lambda_1 T_p. \tag{6}$$

Consequently, the probability of no collision for packet n is given by

$$\text{prob}(\text{packet } n \text{ is collision-free} \mid \text{packet } n \text{ arrived at } t_n) = (1 - 2\lambda_1 T_p)^{N-1}. \tag{7}$$

The FC discards the collisions, buffers the correctly received packets, and waits to have a sufficient number of packets to perform the reconstruction. Let $K(\lambda_1, T)$ denote the number of correctly received packets at the FC during the time interval T. The probability that a packet is fully received within $[T_x, T_x+T]$ and is collision-free is given by

$$q = \lambda_1(T - T_p)\left(1 - 2\lambda_1 T_p\right)^{N-1}. \tag{8}$$

To derive a simple expression characterizing $K(\lambda_1, T)$, we propose the following approximate model for the density function of the number of correctly received packets:

$$P_K(k; \lambda_1, T) = \text{prob}\left(K(\lambda_1, T) = k\right) = B(N, q) = \binom{N}{K} q^k (1-q)^{N-k} \tag{9}$$

Author's personal copy

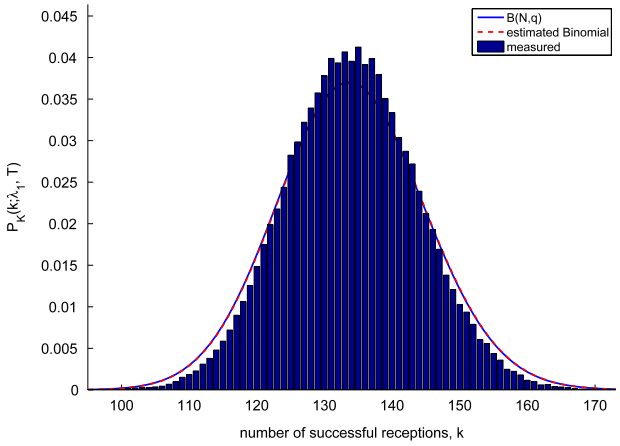

Fig. 4. Probability density function of the number of correctly received packets $K(\lambda_1, T)$ for $N = 1000$, $T = 200$ s, $T_1 = 1000$ s ($\lambda_1 = 1/T_1 = 0.001$ packet/s) and $T_p = 0.2$ s; the number of simulation runs is 100,000.

Table 1
Kullback–Leibler distances between the simulated data and the binomial model in Eq. (9) ($T_p = 0.2$ s and the number of simulation runs is 100,000).

$N = 1000$	$T = 200$ s	$T = 1000$ s
$\lambda_1 = 0.001$ packet/s	0.0141	0.081
$\lambda_1 = 0.0001$ packet/s	0.00092	0.0012

where q is given by Eq. (8). To justify the validity of this simple model, we have conducted simulation experiments. Fig. 4 shows the histogram of the number of correctly received packets obtained from simulation, as well as the plot of $B(N, q)$, where q is determined from Eq. (8), and $B(N, q_{est})$, where q_{est} is estimated from the simulated data. We observe that our approximation for $P_K(k; \lambda_1, T)$ closely matches the estimated binomial and fits the simulated data. Table 1 also shows the Kullback–Leibler distances[1] between the probability distribution of the simulated data and the model in (9) for different values of T and λ_1. Noting a good match, we will rely on this model when we proceed with system design in Section 4.

3.2. Scenario 2: Poisson arrival process

In this scenario, we assume that each node generates packets according to an independent Poisson process at an average rate of λ_1. The nodes transmit their packets as soon as they are generated. The overall packet arrival rate at the FC is $\lambda = N\lambda_1$. In order to be able to reconstruct the field, the FC needs to collect at least N_s useful packets as before; however, unlike in the deterministic scenario, there is no guarantee that the packets received by the FC belong to *different* nodes. Therefore, if the FC receives multiple packets from a node, it keeps only one packet and discards the copies. The FC deals with collisions as before, by simply discarding them. The total number of packets that are used in the reconstruction process, $K(\lambda_1, T)$, is the number of received packets left after discarding the colliding packets *and* the multiple copies of the same packet. Hence, the FC observes an effective arrival rate (successful and non-repeated packets only) that is less than λ, say λ'. We suggest the following model for λ':

$$\lambda' = \frac{N(1 - e^{-\lambda_1 T})e^{-2N\lambda_1 T_p}}{T}. \tag{10}$$

This model can be justified by the following two observations:

(i) Given an arrival rate of $\lambda = N\lambda_1$, the probability of no collision at the FC is modeled as

$$\text{prob(no collision)} = e^{-2N\lambda_1 T_p}. \tag{11}$$

The average number of collision-free packets observed at the FC in T is thus $N\lambda_1 e^{-2N\lambda_1 T}$.

(ii) Focusing on an individual node, let $\mathcal{N}_1(T)$ denote the number of packets that it generates in T. The FC discards repetitive packets; hence, the effective number of packets generated at each node during T is given by

$$\mathcal{N}_1'(T) = \begin{cases} 0, & \mathcal{N}_1(T) = 0 \\ 1, & \mathcal{N}_1(T) \geq 1. \end{cases} \tag{12}$$

The average effective packet generation rate at each node is thus some $\lambda_1' \leq \lambda_1$. Let us define the corresponding reduction factor as $\rho = \lambda_1'/\lambda_1$, i.e.,

$$\rho = \frac{E\left\{\mathcal{N}_1'(T)\right\}}{E\left\{\mathcal{N}_1(T)\right\}} = \frac{1 - \text{prob}\{\mathcal{N}_1(T) = 0\}}{\lambda_1 T} = \frac{1 - e^{-\lambda_1 T}}{\lambda_1 T}. \tag{13}$$

The average arrival rate of useful packets at the FC, λ', can now be expressed as the product of average aggregate arrival rate, the reduction factor ρ and the probability of no collision:

$$\lambda' = N\lambda_1 \rho e^{-2N\lambda_1 T_p}. \tag{14}$$

Substituting for ρ from Eq. (13), the above expression reduces to (10). We now conjecture that $K(\lambda_1, T)$ is modeled as a Poisson process,[2] i.e.,

$$P_K(k; \lambda_1, T) = \text{prob}\left(K(\lambda_1, T) = k\right) = \frac{(\lambda' T)^k}{k!} e^{-\lambda' T} \tag{15}$$

where λ' is given by Eq. (10). In order to examine our conjecture, we conducted numerical experiments. Fig. 5 shows the histogram of a simulated $K(\lambda_1, T)$ process, the Poisson distribution with λ' of Eq. (10), and the Poisson distribution with λ_{est}, an average arrival rate estimated from the simulated data. Table 2 shows the

[1] The Kullback–Leibler distance or the relative entropy between two probability mass functions $p(x)$ and $q(x)$ is defined as [23]

$$D(p \parallel q) = \sum_x p(x) \log_2 \frac{p(x)}{q(x)}.$$

[2] Note that the Poisson model is commonly adopted for analyzing random access protocols [24], where it is assumed that the aggregate packet arrival, including retransmitted packets in case of collisions, follows a Poisson model. Here, we invoke a similar assumption for the total number of packets that remains after we discard the colliding and duplicate packets.

Author's personal copy

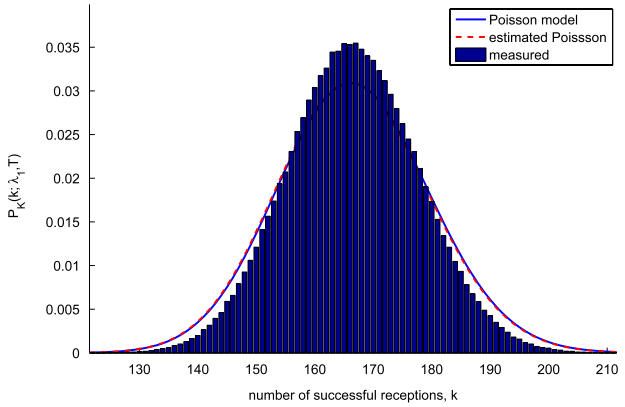

Fig. 5. Probability density function of the number of correctly received packets $K(\lambda_1, T)$ for $N = 2500$, $T = 400$ s, $\lambda_1 = 0.001$ packet/s and $T_p = 0.2$ s; the number of simulation runs is 500,000.

Table 2
Kullback–Leibler distances between the simulated data and the Poisson model in Eq. (15). ($T_p = 0.2$ s and the number of simulation runs is 100,000).

$N = 2500$	$T = 200$ s	$T = 1000$ s
$\lambda_1 = 0.001$ packet/s	0.0248	0.0191
$\lambda_1 = 0.0001$ packet/s	0.0046	0.0117

Kullback–Leibler distances between the distribution of the simulated $K(\lambda_1, T)$ and the model (15) for few values of T and λ_1. Noting a good match between the model and the simulation, we will rely on (15) when we proceed to design the system in Section 4.

4. System design

We propose two design criteria for the sensor network and provide an analytical framework to determine the corresponding design parameters. In the first approach, we aim at minimizing the required recovery time. In this "fast recovery" criterion, the design approach is to fix λ_1, and find the smallest T (denoted by T_s) for which recovery is achieved with a desired probability. In other words, the question that we address is how long does the FC need to wait in order to collect a sufficient number of packets to reconstruct the field. This approach is of interest for applications where recovery time is a major concern. In the second criteria, we aim at minimizing the power consumption in the network. In this "power efficiency" criterion, the design approach is to fix the recovery time T, and find the smallest λ_1 (denoted by λ_{1s}) for which field recovery is achieved with a desired probability. The question now is how often the sensor nodes need to transmit. This approach is suitable for applications where power, i.e., the network lifetime, is a major constraint. The two design approaches thus exhibit a trade-off between recovery time and power efficiency. The choice of the appropriate approach is specific to a particular system's constraints. Note that in both cases, in order for a design to be feasible, the collection time T has to be smaller than or equal to the coherence time (T_{coh}) of the measured process.

For a given system, we define the performance requirement as the minimum *probability of sufficient sensing* P_s. In other words, we ask that the FC collect at least $N_s = CS \log N$ useful packets during time T with probability P_s or higher. This condition can be expressed as

$$\text{prob}\,(K(\lambda_1, T) \geq N_s) \geq P_s. \tag{16}$$

We now seek to obtain the values of system parameters, i.e., T or λ_1, that will satisfy the above sufficient sensing condition. To do so, it will be useful to define the complementary cumulative function of $K(\lambda_1, T)$:

$$\begin{aligned} Q_K(N_s; \lambda_1, T) &= \text{prob}\,(K(\lambda_1, T) \geq N_s) \\ &= \sum_{k=N_s}^{\infty} P_K(k; \lambda_1, T) \\ &= 1 - \sum_{k=0}^{N_s-1} P_K(k; \lambda_1, T) \end{aligned} \tag{17}$$

where $P_K(k; \lambda_1, T)$ is given by Eq. (9) for the deterministic arrival model, or by Eq. (15) for the Poisson arrival model.[3]

4.1. Design criterion 1: fast recovery

Under this criterion, given a fixed λ_1, the goal is to recover the field with probability P_s in the shortest time possible T_s. In other words, we want to determine the value of T_s for which

$$Q_K(N_s; \lambda_1, T_s) = P_s. \tag{18}$$

Eq. (18) can be solved for T_s numerically. Below, we illustrate the fast recovery design approach for the deterministic and the Poisson arrival models. To do so, we use an example of a network consisting of $N = 2500$ nodes and a system design that calls for the probability of sufficient sensing $P_s = 0.9$. The packets have a duration $T_p = 0.2$ s and are generated at a rate of $\lambda_1 = 10^{-3}$ packet/s. We assume that the measured process has a sparse representation in the frequency domain with sparsity $S = 10$. Assuming $C = 2$, $N_s = CS \log N \approx 142$ correctly received packets are required for reconstructing the field.

Deterministic model. The question that we want to answer is how long does the FC need to listen before it can recover the field with the probability $P_s = 0.9$. To answer this question, in Fig. 6(a) we show the complementary cumulative function $Q_K(N_s; \lambda_1, T)$ versus q. This plot is used to find q_s, the value corresponding to P_s. Once this value is determined, Fig. 6(b), which represents Eq. (8), is

[3] Note that for the Poisson model, calculating $(\lambda' T)^k$ may become intractable as k grows. In order to alleviate this problem, in the numerical simulations we use the Gosper approximation for the factorial function [25],

$$k! \approx \sqrt{\left(2k + \frac{1}{3}\right)\pi k^k e^{-k}}$$

which yields the following approximation for the Poisson probability density function

$$P_K(k; \lambda_1, T) \approx \frac{1}{\sqrt{(2k + \frac{1}{3})\pi}} \left(\frac{\lambda' T}{k}\right)^k e^{-\lambda' T + k}.$$

Author's personal copy

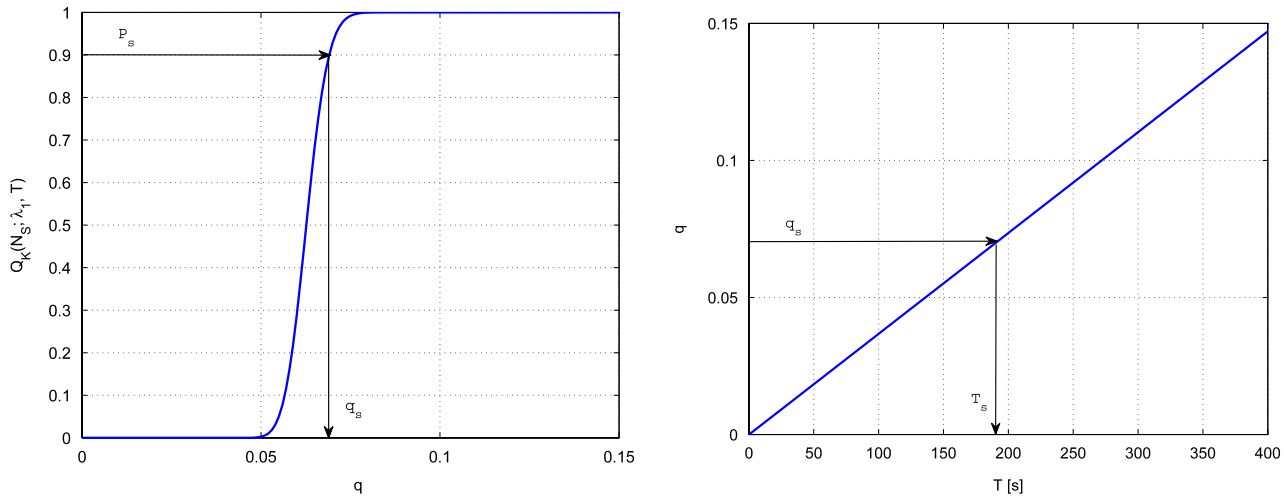

(a) $q_s = 0.07$. (b) $T_s = 191$ s.

Fig. 6. Determining T_s, using the fast recovery criterion, for the example of deterministic arrivals: required probability of sufficient sensing $P_s = 0.9$ implies $q_s = 0.07$ which in turn determines $T_s = 191$ s.

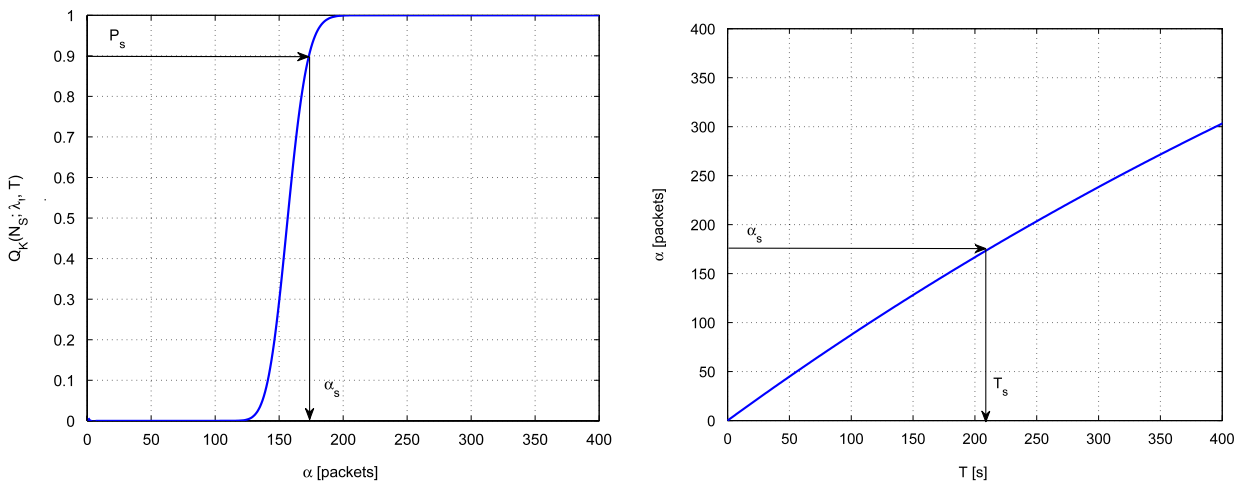

(a) $\alpha_s = 174$. (b) $T_s = 210$ s.

Fig. 7. Determining T_s, using the fast recovery criterion, for the example of Poisson arrivals: required probability of sufficient sensing $P_s = 0.9$ implies $\alpha_s = 174$ which in turn determines $T_s = 210$ s.

used to determine the time required for sufficient sensing. We obtain $T_s = 191$ s; hence, in order to recover the field with probability 0.9, the FC needs to collect packets for at least $T_s = 191$ s.

Poisson model. We consider the same example network, assuming that each node generates a packet according to a Poisson process at an average rate of $\lambda_1 = 10^{-3}$ packet/s. Fig. 7(a) shows $Q_K(N_s; \lambda_1, T)$ versus $\alpha = \lambda' T$. Corresponding to $P_s = 0.9$, this figure implies a value $\alpha_s = 174$. Now, using α_s, Fig. 7(b), which corresponds to Eq. (10), implies $T_s = 210$ s. Note that the value of T_s obtained using a Poisson transmission model is greater than the value of T_s obtained using a deterministic arrival model with the same per node arrival rate. This difference is due to the fact that a Poisson model may result in repetitive packets, hence the FC requires a longer time to obtain the same number of collision-free and repetition-free packets.

4.2. Design criterion 2: power efficiency

Under this criterion, we assume that the system has a specified recovery time $T \leq T_{coh}$. Our goal is to recover the field at minimum packet transmission rate, which translates into minimum power expenditure. The design parameter is thus the minimum sensing rate of each node, λ_{1s}, that needs to be determined such that

$$Q_K(N_s; \lambda_{1s}, T) = P_s. \tag{19}$$

This equation can be solved numerically for λ_{1s}. We illustrate this design approach for both deterministic and Poisson models through our earlier example. The recovery time is now set to $T = 1000$ s, and the arrival rate λ_{1s} is to be determined.

Deterministic model. The question now is how fast does each sensor need to sample the process such that the FC can recover the field with probability $P_s = 0.9$ within T seconds. To answer this question, we show in Fig. 8(a) the complementary cumulative distribution

Author's personal copy

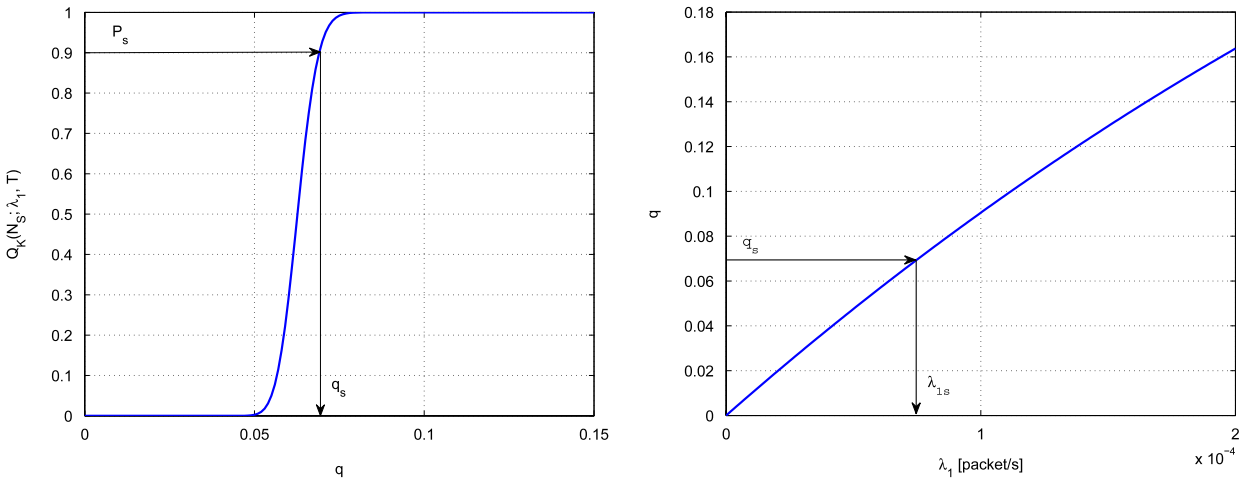

(a) $q_s = 0.07$. (b) $\lambda_{1s} = 7.6 \times 10^{-5}$ packet/s.

Fig. 8. Determining λ_{1s}, using the power efficiency criterion, for the example of deterministic arrivals: required probability of sufficient sensing $P_s = 0.9$ implies $q_s = 0.07$ which in turn determines $\lambda_{1s} = 7.6 \times 10^{-5}$ packet/s.

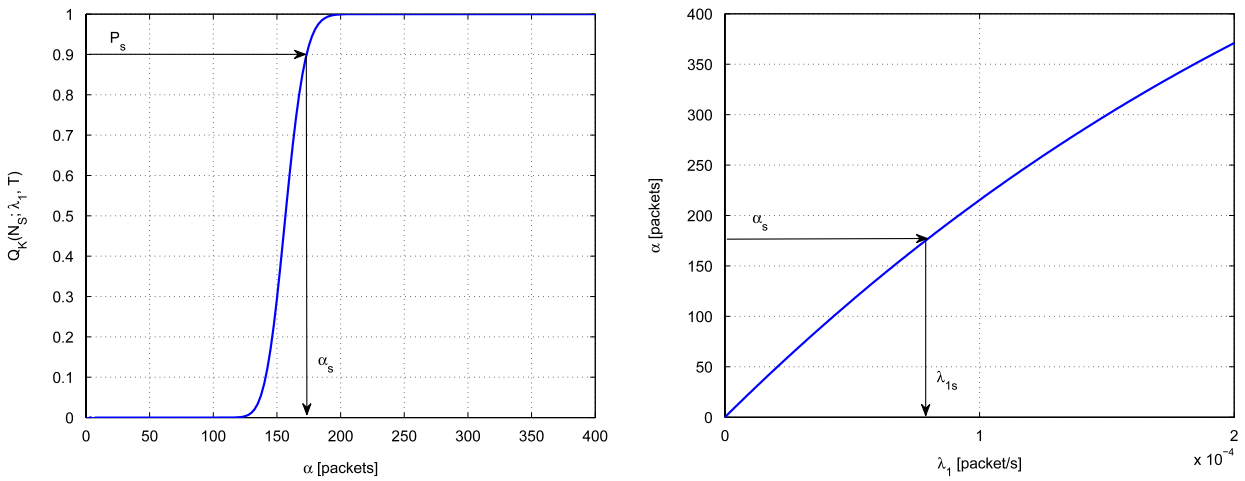

(a) $\alpha_s = 175$. (b) $\lambda_{1s} = 7.9 \times 10^{-5}$ packet/s.

Fig. 9. Determining λ_{1s}, using the power efficiency criterion, for the example of Poisson arrivals: required probability of sufficient sensing $P_s = 0.9$ implies $\alpha_s = 175$ which in turn determines $\lambda_{1s} = 7.9 \times 10^{-5}$ packet/s.

function $Q_K(N_s; \lambda_{1s}, T)$ versus q. Corresponding to the desired $P_s = 0.9$, the underlying probability q is determined as $q_s = 0.07$. For this value, Fig. 8(b), which shows q versus λ_1 using Eq. (8), implies a sensing rate of at least $\lambda_{1s} = 7.6 \times 10^{-5}$ packet/s.

Poisson model. For the specified collection interval $T = 1000$ s, Fig. 9(a) shows $Q_K(N_s; \lambda_{1s}, T)$ versus α. From this figure, the value of α corresponding to P_s is determined as $\alpha_s = 175$. For the so-obtained value of α_s, Fig. 9(b), which shows $\alpha = \lambda' T$ as a function of λ_{1s} according to Eq. (10), implies $\lambda_{1s} = 7.9 \times 10^{-5}$ packet/s. Similarly as in the fast recovery design approach, the packet transmission rate required in the Poisson transmission case is greater than the packet transmission rate required in the deterministic arrival case.

5. Performance analysis

To assess the performance of continuous-time RACS, we consider three criteria: recovery time, total consumed power, and required bandwidth. As a comparison benchmark, we use a conventional network with deterministic sensing and deterministic access. In the conventional network, all N nodes conduct measurements every T seconds and transmit their data packets to the FC using a standard TDMA. This approach requires scheduling, such that packets from different nodes arrive back-to-back at the FC. Fig. 10 depicts the required scheduling process. One frame of data contains N packets, and the total collection time has to be $T = NT_p \leq T_{coh}$. The maximum number of nodes that can be deployed in a conventional network is thus given by $N \leq \frac{T_{coh}}{T_p}$, where T_{coh} is the property of the sensing field. Thus, the coverage area of a conventional network is limited to $A = Nd^2 \leq T_{coh} d^2 / T_p$.

5.1. Time analysis

Fig. 11 compares the collection time needed for each scheme as a function of the number of nodes, i.e., the area covered by the network. The signal is assumed to have

Author's personal copy

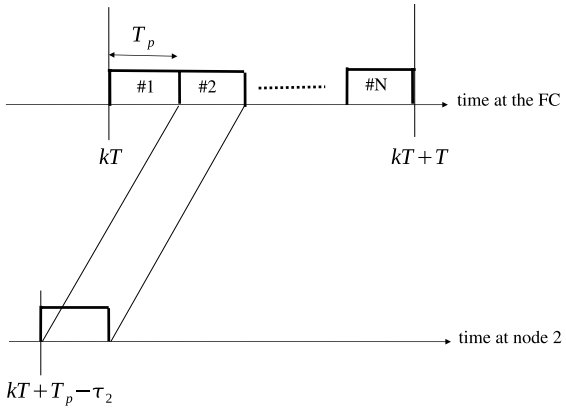

Fig. 10. The scheduling required at each node in the benchmark case (TDMA).

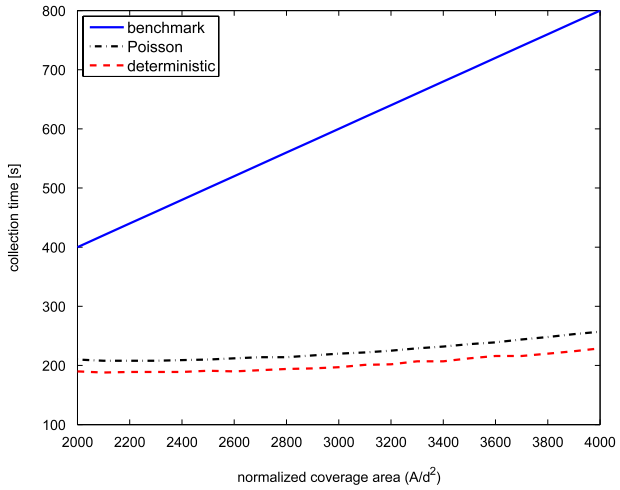

Fig. 11. Collection time vs. network coverage area, under the fast recovery design criterion of Section 4.1; $\lambda_1 = 10^{-3}$ packet/s and $T_p = 0.2$ s.

a fixed sparsity $S = 10$ and the fast recovery design procedure of Section 4.1 is employed. The collection time for the benchmark design is given by $T = NT_p$. We note that RACS offers substantial savings in the collection time as compared to the conventional design. Moreover, the savings grow with the coverage area, as long as the sparsity does not change. For instance, for $N = 2500$ sensor nodes, the collection time of RACS is less than half of that required for a conventional network. Note also that the collection time of the network assuming a Poisson model is slightly greater than the one assuming a deterministic model, which is to be expected due to the occurrence of repetitive packets in the Poisson model.

5.2. Power analysis

We now derive the (average) total transmit power consumption of the network for each of the schemes. Let $\mathcal{P}_1$ denote the transmission power per node required to send a data packet to the FC. For the sake of generality, we assume that all nodes transmit at the same power. The total consumed power in the benchmark (conventional) case, denoted by $\mathcal{P}_c$, is given by

$$\mathcal{P}_c = N\mathcal{P}_1. \tag{20}$$

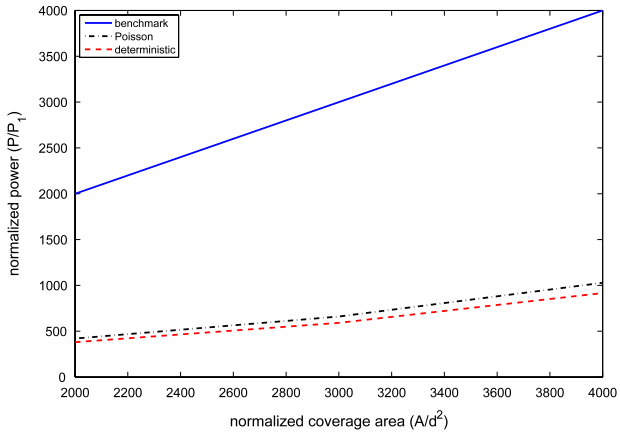

Fig. 12. Total power consumption vs. coverage area, under the power efficiency design of Section 4.2; $T = 1000$ s and $T_p = 0.2$ s.

The coverage area is given by $A = Nd^2$; therefore,

$$\mathcal{P}_c = \frac{A}{d^2}\mathcal{P}_1. \tag{21}$$

The average total consumed power for continuous-time RACS, with deterministic or Poisson arrival models, is given by

$$\overline{\mathcal{P}} = N\lambda_1 T\mathcal{P}_1 \tag{22}$$

where $N\lambda_1 T$ is the average number of nodes that transmit in one collection interval T. The minimum power consumption corresponds to the minimum sensing rate λ_{1s}, which is calculated according to the power efficiency design criterion of Section 4.2. Fig. 12 compares the consumed power by each scheme as a function of the area covered by the network. We note that continuous-time RACS offers substantial savings as compared to the benchmark case. For $N = 2500$, the power consumed by RACS is about 7 dB less than the power consumed by the conventional TDMA network to cover the same area. As before, power consumption is slightly higher if the packets are generated according to the Poisson process as compared to the deterministic process.

5.3. Bandwidth analysis

Bandwidth is severely limited in an underwater acoustic network, hence the lower the bandwidth requirement, the more practical the network scheme is for underwater applications. We define the minimum required bandwidth, B_s, as the bandwidth for which sufficient sensing can be provided, and compare this bandwidth for different schemes.

5.3.1. Benchmark case

In the benchmark scheme, for the network to recover the field within T_{coh}, the frame duration has to be $T = NT_p \leq T_{coh}$, where $T_p = L/B$ and we are assuming for simplicity that B equals the bit rate. Hence, the minimum bandwidth requirement is stated as

$$B \geq \frac{NL}{T_{coh}} = B_s. \tag{23}$$

Author's personal copy

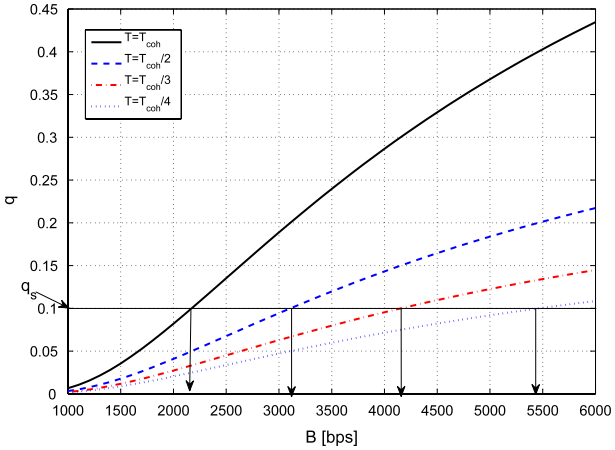

Fig. 13. The probability q of Eq. (8) plotted vs. B for various values of T; $N = 2500$, $T_{coh} = 1000$ s and $L = 1000$ bits.

5.3.2. Continuous-time RACS with deterministic packet arrivals

Fig. 13 shows the probability q as a function of bandwidth B for various values of the collection time T. As seen from the figure, for a certain q_s, the minimum bandwidth usage corresponds to maximum T, $T = T_{coh}$. Hence, in order to determine the minimum bandwidth, we let $T = T_{coh}$. Moreover, we assume that $T_p \ll T_{coh}$; hence, $T_{coh} - T_p \approx T_{coh}$, and

$$q \approx \lambda_1 T_{coh} \left(1 - 2\lambda_1 T_p\right)^{N-1}. \tag{24}$$

Fig. 14 plots this q as a function of λ_1 for a sample set of parameters. In order for a set of design parameters to be achievable, q_s has to be below the maximum value $q_{\max}$; otherwise, no solution for λ_1 exists. Setting the derivative of q with respect to λ_1 equal to zero, we obtain the maximum value of q as

$$q_{\max} = \frac{T_{coh}}{2NT_p}\left(1 - \frac{1}{N}\right)^{N-1} \approx \frac{T_{coh}}{2NT_p e} \tag{25}$$

where the approximation is valid for large N. Now, in order for a solution to exist, $q_s \le q_{\max}$ has to hold. This condition yields the required bandwidth as

$$B \ge \frac{2NLq_s e}{T_{coh}} = B_s. \tag{26}$$

5.3.3. Continuous-time RACS with Poisson packet arrivals

Analogous to the deterministic case, here we can find λ_1 for which λ' of Eq. (10) is maximized. Setting the derivative of λ' with respect to λ_1 equal to zero results in

$$\lambda_1 = \frac{1}{T}\log\left(1 + \frac{T}{2NT_p}\right). \tag{27}$$

Now the maximum value $\lambda'_{\max}$ is given by

$$\lambda'_{\max} = \frac{1}{2T_p}\left(1 + \frac{T}{2NT_p}\right)^{-\frac{2NT_p}{T}-1} \approx \frac{1}{2T_p e} \tag{28}$$

where the approximation holds for $T \ll 2NT_p$, which will normally be justified for large N. Noting that $\lambda'_s \le \lambda'_{\max}$

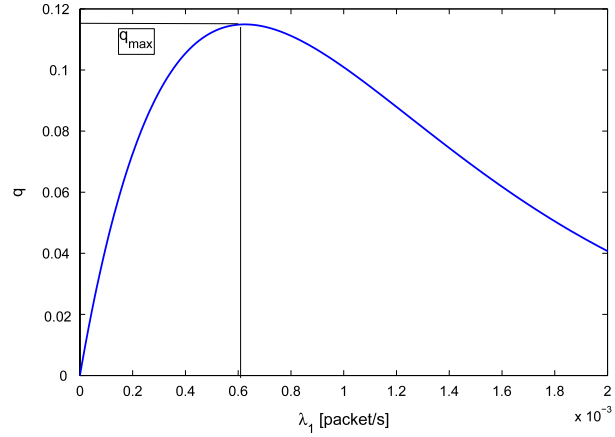

Fig. 14. The probability q of Eq. (24) plotted vs. λ_1 exhibits a clear maximum; $N = 4000$, $T_{coh} = 500$ s and $T_p = 0.2$ s.

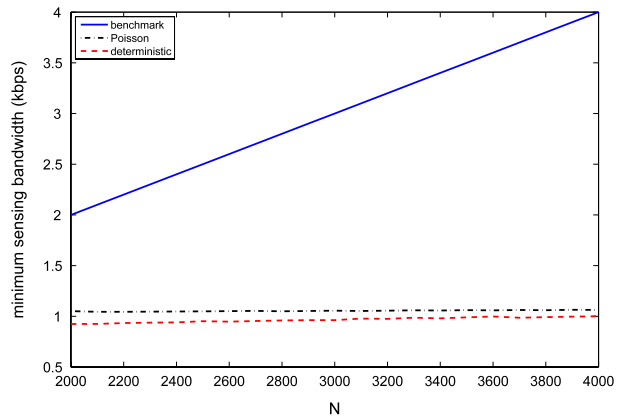

Fig. 15. Minimum bandwidth requirement vs. N.

has to hold in order for the solution to exist, we arrive at the minimum bandwidth requirement:

$$B \ge 2eL\lambda'_s = B_s. \tag{29}$$

Note that in Eq. (29), B_s depends implicitly on the size of the network N, through the parameter λ'_s, which grows logarithmically with N (e.g., if $P_s = 0.5$ then $\lambda'_s = CS \log N$). Fig. 15 shows the minimum bandwidth required for the three schemes. This result demonstrates that continuous-time RACS is capable of providing the same performance as the benchmark case but using a lower bandwidth, a significant feature from the viewpoint of underwater acoustic networking.

5.4. Power and bandwidth savings

So far we have shown that for a given set of system parameters, N, L and T, RACS achieves power and bandwidth savings compared to the benchmark case. In this section, we quantify the performance limits and find closed form expressions for the achievable savings. Without loss of generality, let us focus on a Poisson packet arrival model. Fig. 16 shows λ_{1s} plotted versus the bandwidth B. The minimum required bandwidth B_s is shown in the figure. We note that as the bandwidth increases from the minimum required, the corresponding

Author's personal copy

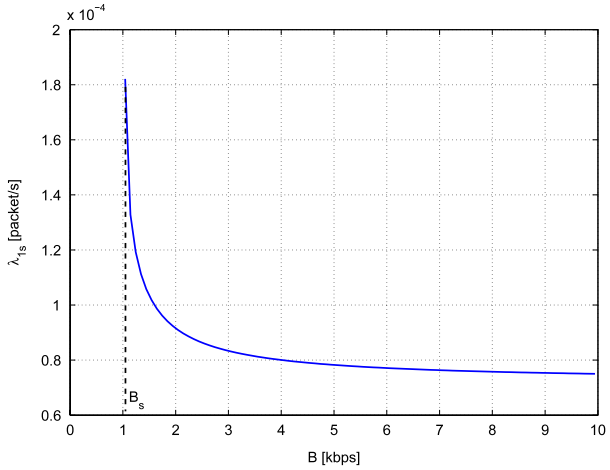

Fig. 16. Minimum per-node sensing rate λ_{1s} plotted vs. the bandwidth B, for $N = 2500$, $N_s = 157$ packets, $L = 1000$ bits and $T = 1000$ s. We note that as the bandwidth increases, the corresponding λ_{1s} decreases.

λ_{1s} decreases, i.e., $\lambda_{1s}(B_s) \geq \lambda_{1s}(B)$. Where, using the expression (27) we have that

$$\lambda_{1s}(B_s) = \frac{1}{T}\log\left(1 + \frac{T}{2NL/B_s}\right). \tag{30}$$

Now, an upper bound on the minimum power, $\mathcal{P}_{up}$, is attained as the power consumption corresponding to $\lambda_{1s}(B_s)$, i.e.,

$$\begin{aligned}\mathcal{P}_{up} &= N\log\left(1 + \frac{T}{2NL/B_s}\right)\mathcal{P}_1 \\ &\approx N\log\left(1 + \frac{e\lambda_s' T}{N}\right)\mathcal{P}_1.\end{aligned} \tag{31}$$

Similarly, from Fig. 16 we note that the smallest λ_{1s} is attained when $B \to \infty$. This value can be derived analytically as

$$\lambda_{1s}(\infty) = \frac{1}{T}\log\left(\frac{1}{1 - \lambda_s' T/N}\right). \tag{32}$$

A lower bound on the average power consumption is thus obtained as

$$\mathcal{P}_{low} = N\log\left(\frac{1}{1 - \lambda_s' T/N}\right)\mathcal{P}_1. \tag{33}$$

The saving in power, $G_{\mathcal{P}}$, offered by employing RACS is thus quantified as

$$\begin{aligned}\mathcal{P}_c/\mathcal{P}_{up} &\approx 1/\log\left(1 + \frac{e\lambda_s' T}{N}\right) \leq G_{\mathcal{P}} \leq \mathcal{P}_c/\mathcal{P}_{low} \\ &= 1/\log\left(\frac{1}{1 - \lambda_s' T/N}\right).\end{aligned} \tag{34}$$

Similarly, the saving in bandwidth, G_B, is derived simply by dividing Eq. (23) by Eq. (29) as

$$G_B = N/2eT_{coh}\lambda_s'. \tag{35}$$

6. Numerical examples

In this section, we use a numerical example to visually illustrate the field recovery process using continuous-time RACS. We consider a 50×50 grid network measuring a physical process with a spatial map given in Fig. 17(a). This map may for instance represent temperature. Its spatial Fourier transform is shown in Fig. 17(b), which indicates a sparse behavior with sparsity $S = 16$. Let us assume a Poisson arrival model for the data packets, a collection time of $T = 1000$ s, and a power-efficient design. Following the design guidelines of Section 4.2, we determine the required sampling rate to be $\lambda_1 = 1.33 \times 10^{-4}$ packet/s. Employing the so-obtained sampling rate, Fig. 18 shows the recovered image at the FC after $T = 1000$ s. We note a good similarity between the original and the recovered map. If by $\mathbf{u}$ we denote the actual data and by $\hat{\mathbf{u}}$ the recovered data, the normalized error ($\frac{\|\hat{\mathbf{u}}-\mathbf{u}\|_{\ell_2}}{\|\mathbf{u}\|_{\ell_2}}$) for the recovered image is on the order of 10^{-9} (-90 dB), which is in the domain of numerical round-off errors. Note that in this example we are considering a noiseless scenario.

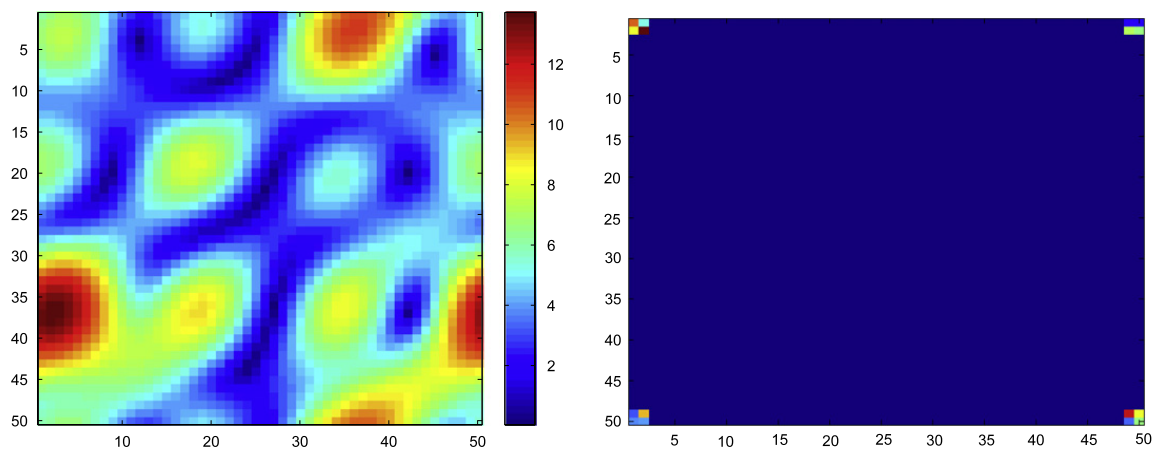

(a) Spatial map of the sensing field.

(b) Spatial Fourier transform of the field.

Fig. 17. The sensing field is sparse in the Fourier domain with $S = 16$.

Author's personal copy

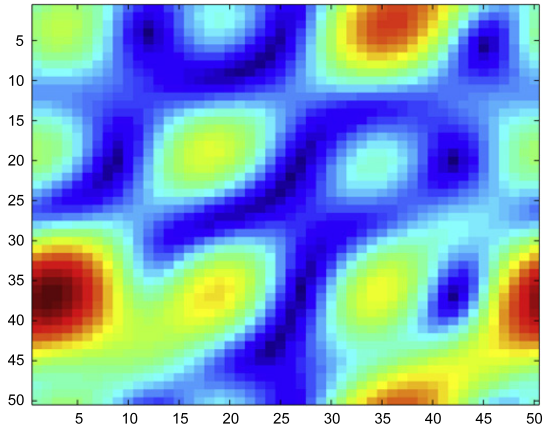

Fig. 18. The spatial map of the field recovered using continuous-time RACS.

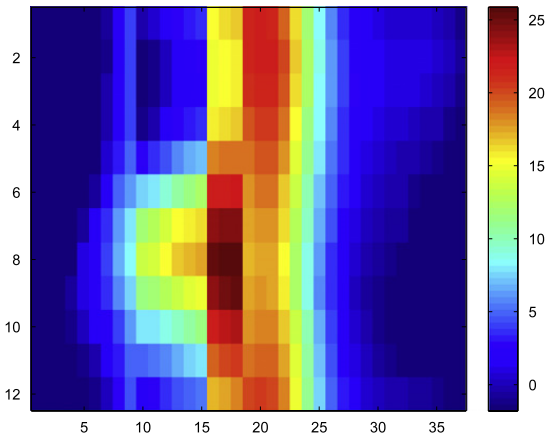

Fig. 19. The spatial map of the sea surface temperature provided by the NOAA/OAR/ESRL PSD, Boulder, Colorado, USA [26].

6.1. Real data example

As an illustrative example, we have used the sea surface temperature data from the National Oceanic and Atmospheric Administration (NOAA) website [26]. This data set contains long term monthly means of sea surface temperatures derived from data taken between the years 1971 and 2000. The network consists of 2.0° latitude by 2.0° longitude global grid spanning 88.0° N–88.0° S and 0.0° E–358.0° E. We use the 12×37 data grid depicted in Fig. 19. The Fourier transform of the data shows a sparse (compressible) representation, where almost 99% of the energy of the signal is contained in $S = 23$ Fourier coefficients. Note that we expect similar sparse behavior models for other natural processes such as deep sea temperature, salinity, etc.

Assuming that each node is capable of transmitting at 10 kbps and that the sea surface temperature is required to be mapped every $T = 5000$ s, for $N_s = 281$, and a probability of sufficient sensing $P_s = 0.9$, the design guidelines of Section 4.2 lead us to $\lambda_1 = 2.41 \times 10^{-4}$ packet/s for the Poisson arrival model. Fig. 20 shows the reconstructed field using the so-obtained λ_1, where the reconstruction error is -20 dB. The recovery error can be reduced further by increasing N_s.

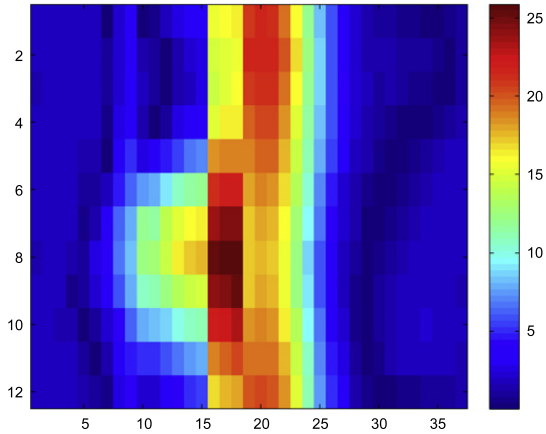

Fig. 20. The recovered map of the sea surface temperature, employing the proposed continuous-time RACS scheme with $\lambda_1 = 2.41 \times 10^{-4}$ packet/s. The corresponding reconstruction error is -20 dB.

7. Conclusion

In this paper, we proposed a networking scheme which combines the concepts of random channel access and compressed sensing to achieve power and bandwidth efficiency, and to eliminate any synchronization or scheduling requirements. The proposed scheme is suitable for large coverage networks, deployed for long-term monitoring of slowly varying phenomena. The design methodology is based on introducing the concept of sufficient sensing probability, i.e., the probability with which the FC is guaranteed to collect a sufficient number of observations ($N_s = CS \log N$). Two design criteria were considered, one that targets a fast recovery, and another that targets power efficiency. Under each criterion, we considered two models for the data packet arrivals, deterministic and Poisson. In each case, we provided design principles for determining the salient system parameters (collection time and packet arrival rate), which ensure that the desired probability of sufficient sensing is met. The benefits of RACS were assessed analytically in terms of the power, time and bandwidth savings achieved over a conventional TDMA scheme. Finally, numerical results were presented to illustrate the effectiveness of the proposed scheme.

References

[1] J. Heidemann, W. Ye, J. Wills, A. Syed, Y. Li, Research challenges and applications for underwater sensor networking, in: Proceedings of the IEEE Wireless Communications and Networking Conference, WCNC, 2006, pp. 228–235.
[2] K. Sohrabi, J. Gao, V. Ailawadhi, G.J. Pottie, Protocols for self-organization of a wireless sensor network, IEEE Personal Communications 7 (2000) 16–27.
[3] C. Schurgers, V. Tsiatsis, S. Ganeriwal, M. Srivastava, Optimizing sensor networks in the energy-latency-density design space, IEEE Transactions on Mobile Computing 1 (1) (2002) 70–80.
[4] W. Wei, J. Heidemann, D. Estrin, An energy-efficient MAC protocol for wireless sensor networks, Proceedings of IEEE Infocom (2002) 1567–1576.
[5] M. Zorzi, P. Casari, N. Baldo, A.F. Harris III, Energy-efficient routing schemes for underwater acoustic networks, IEEE Journal on Selected Areas in Communications 26 (9) (2008) 1754–1766.
[6] F. Zorzi, M. Stojanovic, M. Zorzi, On the effects of node density and duty cycle on energy efficiency in underwater networks, in: Proceedings of IEEE Oceans'10 Asia Pacific Conference, 2010.

Author's personal copy

[7] E.J. Candes, M.B. Wakin, An introduction to compressive sampling, IEEE Signal Processing Magazine (2008) 21–30.
[8] R. Baraniuk, Compressive sensing, IEEE Signal Processing Magazine (2007) 118–121.
[9] W.U. Bajwa, J. Haupt, A.M. Sayeed, R. Nowak, Compressive wireless sensing, in: 5th International Conference of Information Processing in Sensor Networks, IPSN'06, 2006, pp. 134–142.
[10] W. Bajwa, J. Haupt, A.M. Sayeed, R. Nowak, Joint source–channel communication for distributed estimation in sensor networks, IEEE Transactions on Information Theory 53 (10) (2007) 3629–3653.
[11] W.U. Bajwa, A.M. Sayeed, R. Nowak, Matched source–channel communication for field estimation in wireless sensor networks, in: 4th International Conference of Information Processing in Sensor Networks, IPSN'05, 2005, pp. 332–339.
[12] Y. Mostofi, P. Sen, Compressive cooperative sensing and mapping in mobile networks, in: Proceedings of the American Control Conference, ACC, 2009.
[13] A. Griffin, P. Tsakalides, Compressed sensing of audio signals using multiple sensors, in: Proceedings of 16th European Signal Processing Conference, EUSIPCO'08, 2008.
[14] J. Meng, H. Li, Z. Han, Sparse event detection in wireless sensor networks using compressive sensing, in: 43rd Annual Conference on Information Sciences and Systems, CISS, 2009, pp. 181–185.
[15] Q. Ling, Z. Tian, Decentralized sparse signal recovery for compressive sleeping wireless sensor networks, IEEE Transactions on Signal Processing 58 (7) (2010) 3816–3827.
[16] J. Wu, Ultra-low power compressive wireless sensing for distributed wireless networks, in: Military Communications Conference, MILCOM, 2009, pp. 1–7.
[17] S. Hu, J. Tan, Compressive mobile sensing for robotic mapping, in: IEEE International Conference on Automation Science and Engineering, 2008, pp. 139–144.
[18] S. Poduri, G. Marcotte, G.S. Sukhatme, Compressive sensing based lightweight sampling for large robot groups.
[19] A.K. Fletcher, S. Rangan, V.K. Goyal, On–off random access channels: a compressed sensing framework, in revision, IEEE Transactions on Information Theory, available as arXiv:0903.1022.
[20] F. Fazel, M. Fazel, M. Stojanovic, Random access compressed sensing for energy-efficient underwater sensor networks, IEEE Journal on Selected Areas in Communications 29 (8) (2011).
[21] E.J. Candes, J. Romberg, T. Tao, Robust uncertainty principles: exact signal reconstruction from highly incomplete frequency information, IEEE Transactions on Information Theory 52 (2) (2006) 489–509.
[22] A. Syed, J. Heidemann, Time synchronization for high latency acoustic networks, Proceedings of the IEEE INFOCOM (2006) 1–12.
[23] T.M. Cover, J.A. Thomas, Elements of Information Theory, John Wiley & Sons, Inc., 1991.
[24] M. Schwartz, Mobile Wireless Communications, Cambridge University Press, 2005.
[25] E.W. Weisstein, CRC Concise Encyclopedia of Mathematics, second ed, Chapman & Hall, 2002.
[26] http://www.esrl.noaa.gov/psd.

Fatemeh Fazel received the B.S. degree in electrical engineering from the Sharif University of Technology, Tehran, Iran and the M.S. degree from the University of Southern California. She received her Ph.D degree from the Department of Electrical Engineering and Computer Science at the University of California, Irvine in 2008. She is currently a Postdoctoral Associate with the Electrical and Computer Engineering Department at the Northeastern University in Boston. Her research interests are in wireless communications, with a focus on multiple-input multiple-output (MIMO) systems, space–time coding, and energy-efficient sensor networks.

Maryam Fazel received her B.S. degree from the Sharif University, Iran, and her M.S. and Ph.D. degrees from the Stanford University in 2002. She was a postdoctoral scholar and later a Research Scientist in the Control and Dynamical Systems Department at Caltech until 2007. She is currently an Assistant Professor in the Electrical Engineering Department at the University of Washington, Seattle, with adjunct appointments in Mathematics and in Computer Science and Engineering. She is the recipient of a 2009 NSF CAREER Award and an Outstanding Teaching Award at the University of Washington.

Milica Stojanovic (Sm'08, F'10) graduated from the University of Belgrade, Serbia, in 1988, and received the M.S. and Ph.D. degrees in Electrical Engineering from the Northeastern University, Boston, MA, in 1991 and 1993. After a number of years with the Massachusetts Institute of Technology, where she was a Principal Scientist, she joined the faculty of Electrical and Computer Engineering Department at the Northeastern University in 2008. She is also a Guest Investigator at the Woods Hole Oceanographic Institution, and a Visiting Scientist at MIT. Her research interests include digital communications theory, statistical signal processing and wireless networks, and their applications to underwater acoustic communication systems. Milica is an Associate Editor for the IEEE Journal of Oceanic Engineering and the IEEE Transactions on Signal processing.